https://doi.org/10.31925/farmacia.2023.2.15 **ORIGINAL ARTICLE**

DESIGN OF AZITHROMYCIN LOADED EUDRAGIT RL 100 NANOPARTICLES WITH EXTENDED ANTIBACTERIAL EFFECT

IRFAN AKARTAS [1]*, AYSEGUL ATES [2]

[1]*Faculty of Pharmacy, European University of Lefke, Lefke, Turkish Republic of Northern Cyprus, (via Mersin 10, Turkey), Cyprus*
[2]*Department of Pharmaceutical Microbiology, Faculty of Pharmacy, Ege University, Izmir, Turkey*

**corresponding author: iakartas@eul.edu.tr*

Manuscript received: November 2022

Abstract

The main purpose of this study was to prepare Azithromycin (AZM) loaded Eudragit RL 100 (ERL) nanoparticles in order to increase the antibacterial activity of AZM and to compare the drug release profiles of the formulations at the stomach and intestinal pH. AZM-NP-1:5 (AZM:ERL = 1:5) and AZM-NP-1:10 (AZM:ERL = 1:10) nanoparticles were prepared using different drug-polymer ratios. Particle size and zeta potential were analysed and physicochemical characterization was performed using Scanning Electron Microscope (SEM), Fourier Transform Infrared (FT-IR) Spectroscopy, Proton Nuclear Magnetic Resonance (^{1}H-NMR) Spectroscopy, Differential Scanning Calorimetry (DSC) and X-ray Diffraction (XRD). AZM-NP-1:10 have 554.4 ± 29.3 nm size, + 15.4 ± 3.18 mV charge with 77.06 ± 3.63% DL%. In the *in vitro* release tests, after the first 3 hours, 49.35 ± 1.64% of the active ingredient was released from AZM-NP-1:10 at pH 1.2 HCl medium and the release was found to fit Korsmeyer-Peppas kinetic model. A similar release profile (f_2 = 71) of 51.40 ± 1.71% for the first 3 hours was also obtained for AZM-NP-1:10 in PBS at pH 6.8. The Minimum Inhibitory Concentration (MIC) of free AZM and AZM-NP-1:10 against *Staphylococcus aureus* was found to be 2 and 0.5 µg/mL, respectively. The activity of AZM started to decrease after 6 hours while AZM-NP-1:10 presented a continuous antibacterial activity for 24 hours. AZM-NP-1:10 exhibited an enhanced antibacterial activity and a prolonged drug release pattern compared to free AZM, allowing for more effective treatment with fewer side effects.

Rezumat

Scopul principal al acestui studiu a fost de a prepara nanoparticule încărcate cu azitromicină (AZM) și Eudragit RL 100 (ERL), pentru a crește activitatea antibacteriană a AZM și pentru a compara profilurile de eliberare ale formulărilor la pH gastric și intestinal. Nanoparticulele AZM-NP-1:5 (AZM:ERL = 1:5) și AZM-NP-1:10 (AZM:ERL = 1:10) au fost preparate folosind diferite rapoarte medicament-polimer. Dimensiunea particulelor și potențialul zeta au fost analizate și caracterizarea fizico-chimică a fost efectuată folosind microscopul electronic cu scanare (SEM), spectroscopie în infraroșu cu transformată Fourier (FT-IR), spectroscopie de rezonanță magnetică nucleară cu protoni (^{1}H-NMR), calorimetrie cu scanare diferențială (DSC) și difracția de raze X (XRD). AZM-NP-1:10 are dimensiunea de 554,4 ± 29,3 nm, încărcare + 15,4 ± 3,18 mV cu 77,06 ± 3,63% DL%. În testele de cedare *in vitro*, după primele 3 ore, 49,35 ± 1,64% din API a fost eliberat din AZM-NP-1:10 la pH 1,2 și cedarea a fost fitată pe modelul cinetic Korsmeyer-Peppas. Un profil de eliberare similar (f_2 = 71) de 51,40 ± 1,71% pentru primele 3 ore a fost, de asemenea, obținut pentru AZM-NP-1:10 în tampon fosfat la pH 6,8. Concentrația minimă inhibitorie (MIC) de AZM liber și AZM-NP-1:10 împotriva *Staphylococcus aureus* a fost de 2, respectiv 0,5 pg/mL. Activitatea AZM a început să scadă după 6 ore, în timp ce AZM-NP-1:10 a prezentat o activitate antibacteriană continuă timp de 24 de ore. AZM-NP-1:10 a prezentat o activitate antibacteriană îmbunătățită și un model de eliberare prelungită în comparație cu AZM liber, permițând un tratament mai eficient cu mai puține efecte secundare.

Keywords: azithromycin, Eudragit, nanoparticles, antibacterial activity

Introduction

Antimicrobial resistance against antibiotics has become a global health issue in recent years due to both public health impact and economic cost. Multidrug-resistant strains have limited antibiotic options for treatment. According to World Health Organization (WHO), antimicrobial resistance has increased and become emerging as a cause of morbidity and mortality in recent years. These obstacles have created a search for alternative and effective antimicrobial strategies [1, 2]. In the report presented by WHO in 2014, it was stated that if the resistance problem cannot be controlled and the resistance rates continue to increase at this rate, 10 million people will die from infectious diseases due to resistance by 2050 all over the world. WHO stated that this number will rank first, much higher than deaths from cancers, cardiovascular diseases and neurological diseases, and this problem will bring $100 million in additional healthcare expenditure. Resistance is also an important component of global economic loss estimates. It is known that the pharmaceutical industry has problems in developing

new antibiotics due to reasons such as reduced incentives and compelling legal obligations. The number of new antibiotics approved has decreased dramatically, especially in recent years [3-7]. One of the most favourable approaches to overcoming these difficulties is the design of nano-based drug delivery systems. Recent research has shown that the nanoparticles with antibiotics not only reduce the toxicity of both drugs and human cells at lower doses, but also increase their bactericidal effectiveness. To address this issue, innovative approaches to all problems and rational solutions are needed [8]. Nanoparticles are characterized by small particle sizes and high surface areas, which can be advantageous for certain applications due to their absorption. Furthermore, these systems offer numerous benefits including enhanced bioavailability, targeting the molecules, and sustained drug release within the target site [9]. Nanoparticles are promising nanocarriers in increasing the solubility and thus efficacy of hydrophobic drugs. All of these advantages may be able to allow lower dose intake and decrease the side effects [10].

There are many methods for preparing nanoparticles such as solvent evaporation, high-pressure homogenization, nanoprecipitation, salting out, ionic gelation, micro-emulsion, etc. [11, 12]. One of the most commonly used methods for polymeric nanoparticle preparation is the solvent evaporation method. There are two types of techniques used to prepare nanoparticles through solvent evaporation, namely single emulsion and double emulsion. The single emulsion technique includes oil in water (o/w) emulsions, whereas the double emulsion technique involves water in oil in water (w/o/w) emulsions. The solvent evaporation method involves the dissolving of polymers in organic solvents, followed by the addition of a drug. The organic phase is added into an aqueous phase containing a stabilizer. Then, the mixture is homogenized by using a homogenizer or sonicated by a probe sonicator. After that, the mixture is stirred constantly for some time to evaporate the organic solvent and precipitate formed nanoparticles [12-15].

Natural and synthetic polymers are used in the development of nanoparticles. ERL is one of the most frequently used synthetic polymers for nanoparticle preparation. It is a copolymer poly (ethyl-acrylate, methyl-methacrylate and chloro-trimethyl-ammonium-ethyl-methacrylate) that contains 8.8 - 12% of quaternary ammonium groups. Eudragit L is used for enteric coating, but ERL is used for sustained/prolonged release. Due to its swelling ability, it is one of the most popular materials for the controlled release of drugs [12, 13].

AZM is a macrolide antibiotic with a 15-membered macrocyclic lactone ring, which has increased activity against Gram-positive and Gram-negative bacteria including *Staphylococcus aureus*, *Bordetella pertussis*, *Legionella sp.*, *Mycoplasma pneumonia*, *Treponema pallidum*, *Chlamydia sp.* and *Mycobacterium avium.* By binding to the 23s rRNA domain of the 50s ribosomal subunit of the 70s bacterial ribosome, it prevents the elongation of the polypeptide chain and the binding of the tRNA chain [18, 19]. It is a poorly water-soluble drug with 37% oral bioavailability. It performs widespread tissue distribution after oral use and provides a long-term effect by accumulating in phagocytes and showing slow release. Also, due to the long half-life (approximately 6 - 8 hours), and the high tissue concentration, the treatment plan is carried out for a short time (3 - 5 days). Azithromycin has been classified as the most critically important antibiotic by the WHO [20-22]. One of the most challenging problems in eliminating Gram-negative pathogens and enhancing treatment efficiency is entering antibiotics into damaged cells and adjusting the optimum concentration of drugs. The use of nanoparticle drug delivery systems to improve the penetration of anti-biotics into cells is a good strategy to enhance efficacy [17, 18].

The oral route is one of the most popular routes for drug administration to treat a variety of diseases. Compared with intravenous administration, oral administration is safe, comfortable and painless. Due to these properties, it is regarded as an attractive route. In addition, drug concentration in the blood can be prolonged with oral administration in contrast with the intravenous route. Drugs should be fully dissolved in the gastrointestinal fluid before being absorbed into the systemic circulation. However, many of the drugs are insoluble in water, which may cause low bioavailability [19, 20].

The aim of this study was to prepare AZM-loaded ERL nanoparticles to increase the efficacy of the drug and to compare the drug release profiles of the formulations at pH 1.2 and 6.8. For this aim, polymeric nanoparticles of AZM were prepared by the o/w emulsion solvent evaporation method and lyophilized to produce stable and small-sized particles for controlled delivery of the drug. AZM-loaded nanoparticles were characterized, and their drug release profiles were analysed. The antibacterial activity of drug-loaded nanoparticles was evaluated and compared with AZM. Although there are formulation studies of AZM developed with some different Eudragit polymers in the literature [27, 28], no nanoparticle studies have been performed with ERL before, and moreover, the drug release profiles of AZM developed with Eudragit at gastric and intestinal pH have not been compared. Taghe and co-workers developed azithromycin-Eudragit nanoparticles and studied *in vitro* drug release only at pH 7.4 [29]. We anticipate that our study can fill the gap in the literature in this sense and shed light on similar studies.

Materials and Methods

Materials

Azithromycin dihydrate was a kind gift from Ali Raif İlaç Sanayi A.Ş (Istanbul, Turkey). ERL was a kind gift from Evonik Industries (Istanbul, Turkey). Poly (vinyl alcohol) (PVA), methanol, acetonitrile, ammonium acetate and dimethylsulfoxide (DMSO) were purchased from Sigma-Aldrich (Munich, Germany). All other chemicals and reagents were of analytical grade.

Preparation of AZM-loaded ERL nanoparticles

Blank nanoparticles (Blank-NP) and AZM-loaded nanoparticles (AZM-NP) with different ratios of AZM: ERL (1:5 and 1:10) were prepared using the single emulsion-solvent evaporation method. AZM and ERL were dissolved in methanol under a magnetic stirrer at 600 rpm for 2 hours at room temperature. PVA was dissolved in distilled water by using an ultrasonic bath for 30 minutes to obtain a 1.25% (% w/v) clear solution. AZM-ERL solution was then placed in an insulin syringe and added dropwise to 20 mL of 1.25% (% w/v) PVA solution under stirring at 900 rpm. Stirring was continued for 10 minutes. Samples in a beaker were sunk in an ice bath and homogenized using a high-speed homogenizer (Digital Ultra Turrax, Germany) at 15,000 rpm for 10 minutes. The oil-in-water (O/W) emulsion was gently stirred at room temperature overnight to evaporate methanol. The mixture was then centrifuged at 13,500 rpm for 15 minutes. The supernatants were removed, then the collected nanoparticles were washed three times with distilled water using the same centrifugation operation previously described. Nanoparticles were then lyophilized using a freeze dryer (Alpha 1–2 LD plus, Martin Christ, Germany) at -50°C, 0.10 mBar for 48 hours.

Determination of particle size, polydispersity index (PDI) and zeta potential

Particle size and PDI values of AZM nanoparticles and Blank-NP were analysed by Photon Correlation Spectroscopy (PCS) using Malvern Nano-ZS (Malvern Instruments, England). Zeta potential was measured using a disposable zeta cuvette by the same instrument. Each measurement was done in triplicate after dispersing nanoparticles in distilled water at 25°C.

Determination of AZM by high-performance liquid chromatography (HPLC)

For the estimation of drug loading and *in vitro* release studies, an HPLC method was used and validated for precision, accuracy and linearity. In this HPLC (Shimadzu, Japan) system, a photodiode array (PDA) detector was used. The method was performed using ACE-5 C18 250 x 46 mm HPLC column (ACE, UK) with an isocratic mobile phase of ammonium acetate (30 mmol/L):acetonitrile (18:82 v/v) at 60°C column temperature. The flow rate of the mobile phase was 1 mL/min and a constant amount of 20 µL was injected by an automatic injector. The wavelength was adjusted to 210 nm. A stock solution of AZM with a concentration of 1000 µg/mL was prepared in DMSO. Dilutions were performed with the mobile phase by using the stock solution and different concentrations of samples were prepared. After that, samples were injected into the chromatographic system and a calibration curve was drawn.

Drug loading efficiency of AZM nanoparticles

To determine the AZM content, nanoparticles were dissolved in DMSO and determined by HPLC by a validated method previously described [30]. Briefly, 10 mg of AZM-loaded nanoparticles (AZM-NP-1:5 and AZM-NP-1:10) were dissolved in 10 mL DMSO under ultrasonic agitation for 10 minutes separately. After vortexing, 100 µL of the mixture was withdrawn and 900 µL of methanol was added to this mixture. The obtained samples were filtered through a 0.2 µm membrane filter and injected into an HPLC system. AZM concentrations in the samples were determined using a calibration curve. The percent drug loading (DL%) (% w/w) of the nanoparticles was calculated by using the equation below (Equation 1). Experiments were repeated three times for each sample.

$$DL\% = 100 \times \frac{\text{entrapped drug in nanoparticles}}{\text{weight of nanoparticles}}, \text{ (Equation 1).}$$

Morphology of nanoparticles

The morphology and structure of AZM and AZM nanoparticles were examined by scanning electron microscopy (SEM), FEI Quanta FEG 650 SEM (Hillsboro, OR, USA). Samples were coated with gold, and the analysis was performed under a high vacuum. SEM images were taken at 50000x magnification, and the nanoparticles below 1 µm were examined.

Thermal analyses of nanoparticles by differential scanning calorimetry (DSC)

The thermograms of AZM, ERL, Blank-NP and AZM nanoparticles were obtained by differential scanning calorimetry (DSC) using DSC-60 (Shimadzu, Japan) between 30°C and 500°C. The samples (5 ± 0.1 mg) were weighed into the aluminium pans separately and sealed hermetically. The analysis was performed under nitrogen gas with a flow rate of 50 mL/min and a heating rate of 10°C/min.

X-ray diffraction (XRD) analyses of nanoparticles

XRD analyses of AZM, Blank-NP and AZM nanoparticles were performed using PANalytical EMPYREAN XRD (Almelo, The Netherlands) in the range of 2 - 40°C with a 2°C/min scanning rate.

Fourier Transform Infrared (FTIR) Spectroscopy

FTIR spectra of AZM, ERL, AZM nanoparticles and Blank-NP were taken using Shimadzu FTIR-8300 (Japan) at the wavelength range of 4000 - 400 cm^{-1}. The samples were analysed in solid form by placing them directly on the ATR crystal.

Proton nuclear magnetic resonance (^{1}H-NMR) spectroscopy

^{1}H-NMR analyses were performed using Varian Mercury-plus AS-400 NMR (Agilent, USA). AZM

nanoparticles and Blank-NP were prepared by dissolving in deuterated DMSO (DMSO-D6).

In vitro release studies and kinetics of AZM and AZM nanoparticles

In vitro release study was performed for AZM and AZM nanoparticles in both pH 1.2 HCl buffer and pH 6.8 phosphate buffer saline (PBS). Briefly, 2 mg AZM, 2.59 mg AZM-NP-1:10 (containing 2 mg AZM) and 3.05 mg AZM-NP-1:5 (containing 2 mg AZM) were placed in a dialysis bag (molecular weight cut-off 12 - 14 kDa) with 1 mL of dissolution medium separately and locked at both ends by clamps. The dialysis bag was then placed separately into the beakers containing 100 mL of 0.1 N HCl buffer (pH 1.2) and 100 mL of pH 6.8 PBS as the dissolution medium and stirred at 37 ± 0.5°C at 150 rpm. 1 mL of dissolution medium was withdrawn at detected time intervals (0.5, 1, 2, 3, 4, 5, 6, 8, 12, 24 hours) and the same amount of fresh medium was added for each time to ensure the sink conditions. The withdrawn samples were tested by the validated HPLC method previously described. The *in vitro* drug release results were analysed for release kinetics. Experiments were performed in triplicate (n = 3).

Storage stability

The storage stability test was carried out to examine the physicochemical stability and the degradation of the drug in the nanoparticle-based systems under storage conditions. Stability tests were carried out in climate cabinets at 30 ± 2°C/65% relative humidity (RH) ± 5% RH for 6 months regarding international guidelines [31]. The storage stability of AZM-NP-1:10 was calculated with the procedure described by Paramera *et al*. with slight modifications. Briefly, 10 mg of AZM-NP-1:10 was dissolved in 10 mL DMSO under ultrasonic agitation for 10 minutes. The sample was vortexed vigorously for 15 minutes and kept at room temperature for 1 hour. The supernatant was filtered and AZM content was determined by HPLC [32]. The characteristics of the nanoparticles were explored using particle size, PDI and zeta potential analysis. Experiments were carried out in triplicate (n = 3).

Antibacterial activity evaluation of AZM and nanoparticles

Staphylococcus aureus ATCC 29213 was used in this study. The bacteria were stored in Brain-Heart Infusion Broth (Merck, Germany) with 10% (% v/v) glycerol at -80°C. The antibacterial activity of AZM, AZM-NP-1:10 and Blank-NP was determined using the broth microdilution method. Minimum inhibitory concentrations (MICs) of AZM and nanoparticles were determined according to the European Committee on Antimicrobial Susceptibility Testing (EUCAST) rules. Mueller-Hinton Agar (MHA) (Merck, Germany) was used for bacterial growth at 37°C for 24 h. Then, *S. aureus* ATCC 29213 was suspended in saline. Bacterial inoculum was fixed to 0.5 McFarland turbidity and the suspensions were diluted 100-fold. Mueller-Hinton broth (MHB) (Merck, Germany) (50 µL) was added to each well of sterile 96-well microdilution plates for bacteria. Suspensions of samples were prepared in sterile distilled water. Stock solutions were adjusted to 8192 µg/mL. Two-fold dilution of samples from 2048 µg/ml to 2 µg/mL was done using micro-plate technique. Bacterial inoculum was added to each well of the plate with the amount of 50 µL, and the plates were incubated at 37°C for 24 h. Growth control for the bacteria and sterility control for the media were also tested. The lowest concentration that inhibits microbial growth is defined as MIC. Experiments were carried out in triplicate (n = 3).

Time-kill assay

The time-kill assay demonstrates the time-dependent antibacterial activity of AZM, AZM-NP-1:10 and Blank-NP. MIC values obtained by the broth micro-dilution method were used in the time-kill assay. Formulations were diluted separately with MHB medium in tubes to prepare MIC, MIC/2 and MIC/4 concentrations. Bacterial inoculum suspensions were adjusted to 10^5 CFU/mL. The control tube and the other tubes containing the formulation were inoculated with bacteria. The tubes were incubated in a shaker incubator at 200 rpm, 37°C. 50 µL samples of culture media were withdrawn and diluted with saline, then plated onto Tryptic Soy Agar (TSA) separately at the predetermined time intervals (0, 4^{th}, 6^{th} and 24^{th} hours). The inoculated TSA mediums were incubated at 37°C, for 24 hours. After incubation, the bacterial colonies were counted by the agar plate count method. The number of viable bacteria was calculated as CFU/mL [33]. These values were converted to logarithmic values and a time-kill curve was created. Experiments were carried out in triplicate (n = 3).

Statistical analysis

Each experiment was carried out three independent times and the data are presented as mean ± standard deviation (SD). The statistical significance of the differences in particle size, zeta potential values, PDI and DL% between the nanoparticle formulations and differences in AZM content (% w/w) between periods in storage stability were tested by one-way analysis of variance (ANOVA). Microsoft Excel and DDSolver add-in program was employed for the *in vitro* release kinetics, similarity factor (f_2) and dissimilarity factor (f_1) calculations. Differences between the evaluated values were considered statistically significant at a level of $p \leq 0.05$.

Results and Discussion

Determination of AZM by high-performance liquid chromatography (HPLC)

The aim of this study was to prepare AZM-loaded ERL nanoparticles in order to increase the efficacy of drug and to compare the drug release profiles of the formulations at stomach and intestinal pH. For

this purpose, the HPLC method was developed and validated for the quantification of AZM in the first step. The HPLC method was determined as precise for repeatability and accuracy (n = 3). The method was determined as repeatable with a residual standard deviation (RSD) < 2 % (n = 6). Linearity was determined at a concentration range of 10 - 250 µg/mL. The method was linear between this range and the calibration curve was described with the equation Y = 1002.2X + 247.3 and the coefficient of determination R^2 = 1. The accuracy and repeatability data for the HPLC method of AZM were shown in Table I. The limit of detection (LOD) and limit of quantification (LOQ) were calculated as 0.29 and 0.90 µg/mL respectively.

Table I

The accuracy and repeatability data for the HPLC method of AZM

Concentration (µg/mL)	%AZM for Accuracy (AVG ± SD)	%AZM for Repeatability (AVG ± SD)
25	99.508 ± 1.003	-
50	100.818 ± 1.091	100.327 ± 1.059
100	100.898 ± 1.182	-

*AVG: average; SD: standard deviation

Physicochemical characterization and drug loading of nanoparticles

Nanoparticles were prepared by solvent evaporation method with two different drug:polymer ratios to analyse the effect of the amount of AZM on drug loading. Particle size, PDI, zeta potential and DL% (% w/w) values of Blank-NP, AZM-NP-1:5 and AZM-NP-1:10 are shown in Table II. Drug:polymer ratio was found to affect drug loading capacity. According to the literature, the reason for the higher drug loading efficiency of AZM-NP-1:10 can be explained by the higher polymer ratio [34]. There is no statistically significant difference between the average particle size of AZM-NP-1:5 and Blank-NP ($p > 0.05$). On the other hand, the average particle size of AZM-NP-1:10 was found to be increased. This situation can be associated with the increase in the polymer amount, which is used during the preparation process. In another study by Patil and Dhawale, the mean particle size of ritonavir-loaded ERL100 nanoparticles increased with the increase of polymer ratio [35]. PDI value indicates the particle size distribution of the dispersion. According to the PDI results, AZM-NP-1:5 and AZM-NP-1:10 have better homogeneity in particle size distribution than Blank-NP. Choi *et al*. stated in a study that a PDI value greater than 0.7 indicates a very broad size distribution of particles [36]. All PDI values of nanoparticles were found in the acceptable range. As a result of statistical studies, no significant difference was observed between the PDI values of AZM-NP-1:5 and AZM-NP-1:10 ($p > 0.05$). Zeta potential provides data about the surface charge of nanoparticles. Zeta potential points out the net electrostatic charge on the surface of the particle and it is an important factor in the evaluation of nanoparticle stability [37, 38]. Higher zeta potential values, either positive or negative provide stability and prevent the aggregation of nanoparticles [39]. The positive charge of nanoparticles can be associated with the cationic structure of ERL polymer [40]. The zeta potential values of Blank and AZM nanoparticles indicate compatibility with the literature data. There is no statistically significant difference between zeta potential values of Blank-NP and AZM nanoparticles ($p > 0.05$). Subsequent experiments were carried out with AZM-NP-1:10 which was chosen as the main formulation because it had a higher DL%.

Table II

Particle size, PDI, zeta potential and DL% (% w/w) values of nanoparticles (n = 3)

Formulation	Particle Size (nm)	PDI	Zeta Potential (mV)	DL% (% w/w)
Blank-NP	392.3 ± 34.7	0.592 ± 0.07	+19.3 ± 3.00	-
AZM-NP-1:10	554.4 ± 29.3	0.387 ± 0.11	+15.4 ± 3.18	77.06 ± 3.63
AZM-NP-1:5	394.1 ± 30.7	0.452 ± 0.07	+17.6 ± 2.56	65.50 ± 2.78

*Blank-NP: Placebo nanoparticles; AZM-NP-1:10: Azithromycin loaded nanoparticles with 1:10 (drug:polymer) ratio; AZM-NP-1:5: Azithromycin loaded nanoparticles with 1:5 (drug:polymer) ratio

Morphology of nanoparticles

The surface morphology of AZM and AZM-NP-1:10 were explored by using SEM. SEM images of AZM and AZM-NP-1:10 were shown in Figure 1. AZM-NP-1:10 nanoparticles prepared were nanometric sized, spherical in shape with some agglomerated particles and had a porous surface. These pores could provide the release of encapsulated AZM. The average sizes ranged between 449-642 nm in diameter for nanoparticles and 1.4 - 2.9 µm for AZM particles. Agglomeration of nanoparticles may have been observed due to the adhesive nature of the polymer and the drying process [41]. The SEM images clearly showed the reduction of particle size for AZM during the nanoparticle development process. Hari *et al*. developed Efavirenz-loaded Eudragit-E100 nanoparticles and characterized their particle size and morphology by low angle light scattering technique and SEM analysis respectively. In the SEM analysis, it was confirmed that the active substance was seen as flakes, while in the form of nanoparticles, the flakes become smaller and encapsulated within the nanoparticles. The reduction

in the particle size of the active substances during the nanoparticle development stage is similar to our study [42].

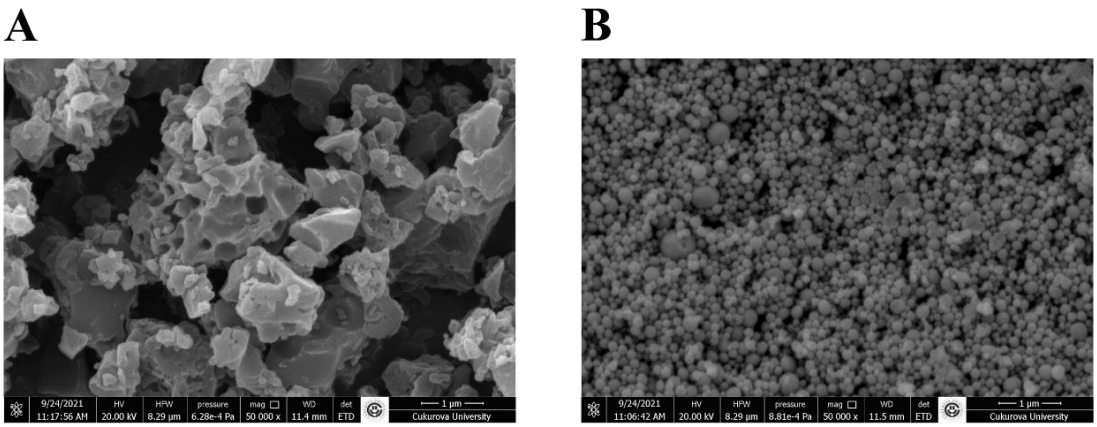

Figure 1.
SEM image of AZM (A) and AZM-NP-1:10 (B) at 1 µm scale

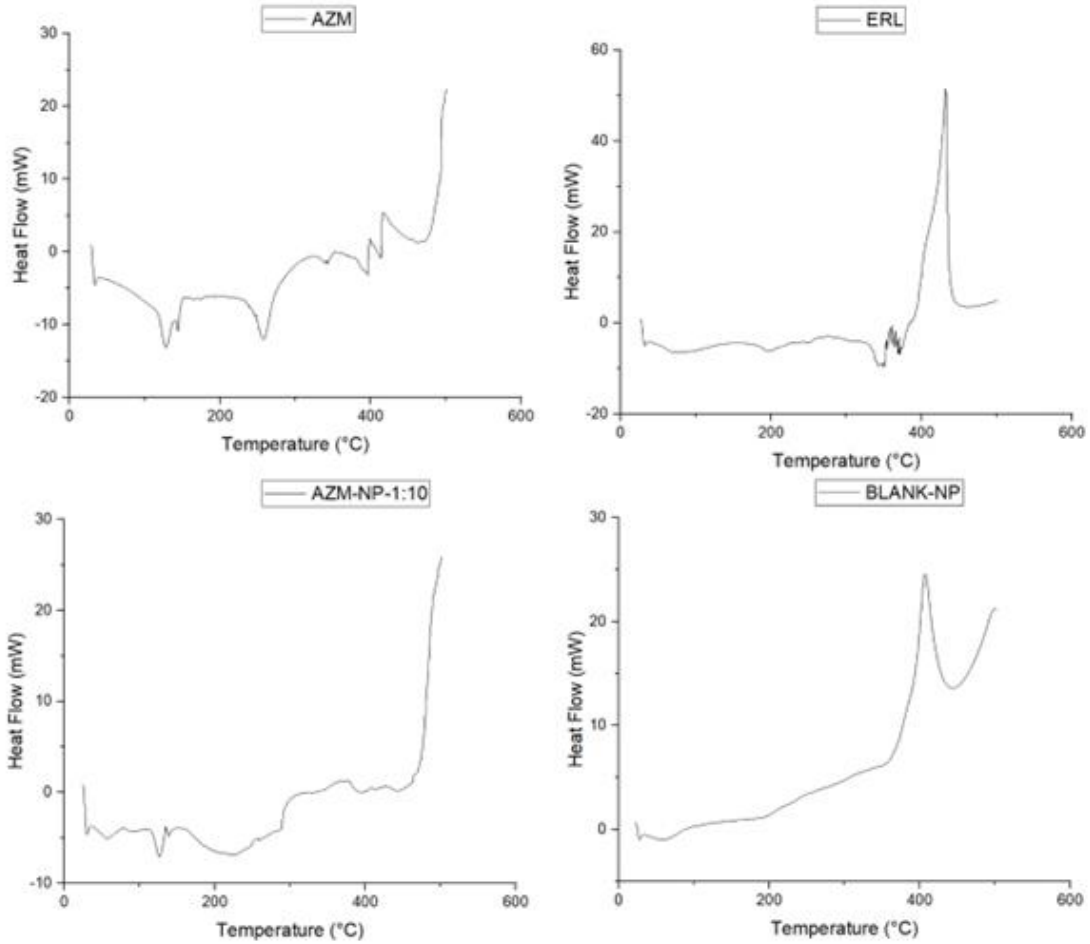

Figure 2.
DSC thermogram of AZM, ERL, AZM-NP-1:10 and BLANK-NP

Thermal analysis of nanoparticles by differential scanning calorimetry (DSC)

DSC analysis was performed to investigate the thermal behaviour and crystallinity of nanoparticles. The DSC thermograms of AZM, ERL, Blank-NP and AZM-NP-1:10 were presented in Figure 2. According to Figure 2, the AZM sample has two endotherms. The first endotherm, which is in the temperature range of 116 - 150°C corresponds to the dehydration step. The DSC thermogram of ERL showed the amorphous

nature of this polymer and no endothermic peaks were detected. When the AZM-NP-1:10 thermogram was examined, it was observed that the enthalpy between 116°C and 150°C in the AZM thermogram further decreased and the anhydrous AZM peak disappeared at 257°C. As a result of AZM's DSC analysis, a thermogram with 2 endotherms was obtained. The first endotherm shows the fusion of the dihydrate group in the drug and the recrystallization of the anhydrous phase. For the first endotherm, the temperature range value was found similar to a study reported by Timoumi *et al*. [43]. The second endotherm step indicates the melting of the anhydrous form of the drug at 257°C. When the AZM-NP-1:10 thermogram was examined, the disappearance of the AZM peak at 257°C indicates that AZM was loaded into the polymeric matrix successfully. The indistinct peak between 116°C and 150°C in the AZM-NP-1:10 thermogram could be justified by the presence of few amounts of AZM on the nanoparticle surface. The decrease and disappearance of drug enthalpies in the thermogram of AZM-NP-1:10 due to the encapsulation of the drug in the polymer matrix was similarly reported in the studies of Koopaei *et al*. and Gambhire *et al*. [44, 45].

X-ray diffraction (XRD) analyses of nanoparticles

XRD analysis is used to reveal the structure of a molecule, confirm the phase state, and obtain data about polymorphism [46]. Figure 3 represents XRD patterns of AZM (**A**), Blank-NP (**B**) and AZM-NP-1:10 (**C**). AZM showed numerous peaks at a diffraction angle (2 θ) of 7.75°, 9.22°, 9.63°, 9.74°, 11.87°, 11.94°, 16.26° and 18.63° with high intensity and sharpness demonstrating its crystalline nature. On the other hand, the diffraction patterns of Blank-NP and AZM-NP-1:10 did not exhibit any sharp peaks. According to the XRD pattern of AZM-NP-1:10, the disappearance of characteristic XRD peaks of AZM indicated the amorphous form of the drug in nanoparticles. These results confirmed that AZM was encapsulated successfully with ERL. In similar results found in the literature, it was stated that the characteristic losartan XRD peaks disappeared in the self-micro emulsifying drug delivery system of losartan [47]. Kumar *et al*. revealed the absence of characteristic peaks of atorvastatin calcium in the XRD pattern of atorvastatin calcium encapsulated Eudragit nanoparticles [48].

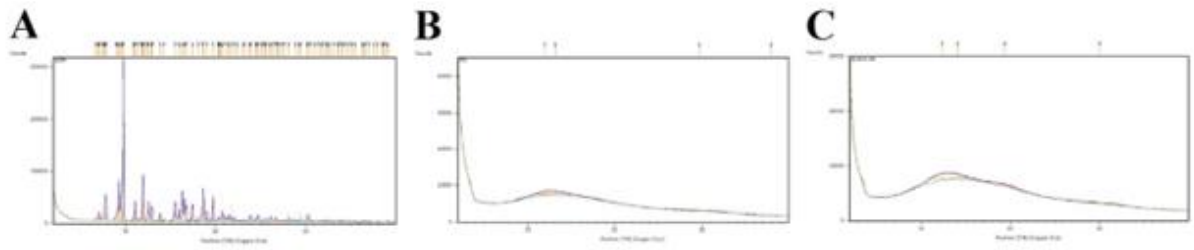

Figure 3.
XRD pattern of AZM (**A**), Blank-NP (**B**) and AZM-NP-1:10 (**C**)

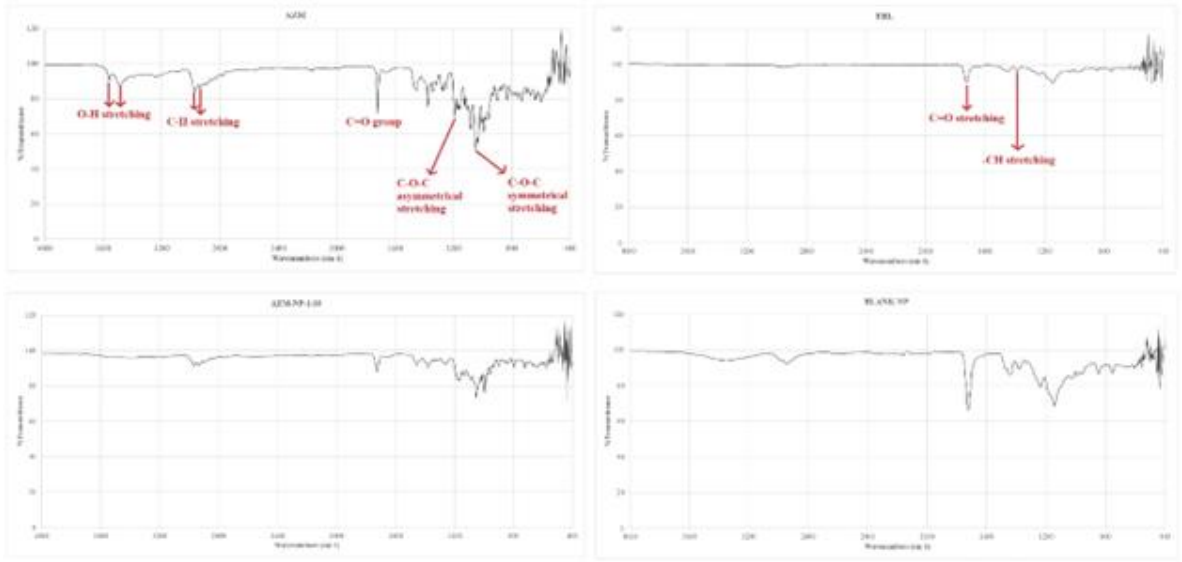

Figure 4.
FTIR spectra of AZM, ERL, AZM-NP-1:10 and BLANK-NP

Fourier transform infrared spectrophotometry (FTIR) analyses

FTIR analyses were used to determine chemical interactions between the drug and the polymer. FTIR spectra of AZM, ERL, AZM-NP-1:10 and Blank-NP are given in Figure 4. According to the spectra of AZM, the peaks at 3558 and 3485 cm^{-1} belong to O-H stretching. The peaks at 2970 and 2933 cm^{-1} correspond to C-H stretching. A strong sharp signal at 1718 cm^{-1} shows the C=O group of AZM. The peaks at 1188 cm^{-1} (C-O-C asymmetrical stretching) and 1047 cm^{-1} (C-O-C symmetrical stretching) are the characteristic peaks of AZM. A strong C=O stretching peak at 1720 cm^{-1} belongs to the carboxylic acid group of ERL in the spectra of ERL. In addition, a weak -CH_3 stretching peak was observed at 1375 cm^{-1} [49]. When compares with FTIR spectra of AZM, due to the absence of new functional group peaks or chemical shift in AZM-NP-1:10 spectra it could be stated that there is no chemical interaction between AZM and ERL polymer [43, 44]. Similar spectrums were obtained for ERL and Blank-NP spectra. However, peak sharpness was observed to be lower in ERL. The characteristic AZM peaks in AZM spectra were observed with significantly lower intensity in AZM-NP-1:10 spectra. This indicated that AZM was encapsulated in the polymeric nanoparticles.

Proton nuclear magnetic resonance (^{1}H-NMR) analyses

The ^{1}H-NMR analysis is used to determine the basic chemical structure of substances, physico-chemical properties and interactions of the drug, polymer and nanoparticles [52]. In this study, ^{1}H-NMR analysis was performed to determine the encapsulation of drugs in a polymer and the interaction between the drug and the polymer. ^{1}H-NMR spectrums of Blank-NP and AZM-NP-1:10 were illustrated in Figure 5A and Figure 5B respectively. According to Figure 5A, a sharp peak at 2.48 belongs to the $(CD_3)_2SO$ solvent and the doublet peak at 3.53 corresponds to the CH_3-OCO- group. Besides, this doublet peak is visible at 3.53 in Figure 5B. In Figure 5B, the peak at 4.73 corresponds to the $(CH_3)_2$CH-OH group. The signal at 4.14 belongs to the tert-buthyl alcohol group in AZM. The signals at 2.89, 3.00, 3.34 and 3.63 correspond to the interaction between the amine group of AZM and the acid group of ERL. According to the obtained ^{1}H-NMR results, due to the formation of CH3-N-, -CH2-N- and -CH-N- peaks could be interpreted by the encapsulation of AZM with ERL. In a study by Tung *et al*., similar interaction peaks between AZM and ERL were observed [53].

In vitro release studies and kinetics of AZM and AZM nanoparticles

In vitro release studies have significance for the quality of the final product. In addition, several mechanisms such as swelling, erosion, stress relaxation of polymers, etc. affect drug release from polymers [54, 55]. The dialysis bag method was used to demonstrate the release profile of the drug and nanoparticles. *In vitro* release profiles of AZM, AZM-NP-1:5 and AZM-NP-1:10 at pH 1.2 HCl and pH 6.8 PBS media are shown in Figure 6. All the nanoparticle formulations showed slower drug release in comparison with AZM. At pH 1.2 medium, 83.59 ± 1.92% of AZM was released in the first 3 hours, while 87.07 ± 2.00% was released at pH 6.8. On the other hand, AZM-NP-1:5 and AZM-NP-1:10 showed 36.32 ± 1.92 and 49.35 ± 1.64% drug release in the same period at pH 1.2 medium. At pH 6.8, the release values of AZM-NP-1:5 and AZM-NP-1:10 are 37.83 ± 2.00 and 51.40 ± 1.71%.

The comparison of *in vitro* dissolution profiles of formulations at pH 1.2 and pH 6.8 was made by calculating f_1 and f_2 values. In order to say that two different *in vitro* dissolution profiles are similar to each other, f1 should be between 0 and 15 whereas f2 should be between 50 and 100 [56]. In the light of the release profiles obtained, f_1 and f_2 values were calculated as 7 and 62 for AZM, 6 and 74 for AZM-NP-1:5 and 6 and 71 for AZM-NP-1:10, respectively.

The *in vitro* release data were fitted with different mathematical drug release models including zero order, first order, Higuchi, Hixson-Crowell, Hopfenberg, Peppas-Sahlin and Korsmeyer-Peppas models. *In vitro* drug release data were entered into the DDSolver program to calculate the coefficient of determination (R^2), adjusted coefficient of determination ($R^2_{adjusted}$), Akaike Information Criterion (AIC) and Model Selection Criterion (MSC). The model with the highest R^2, $R^2_{adjusted}$, MSC and the lowest AIC was selected as the best model [57]. When the release profiles in pH 1.2 HCl medium are examined, among all release models, the first order was the best fitted kinetic model for AZM, Peppas-Sahlin for AZM-NP-1:5 and Korsmayer-Peppas for AZM-NP-1:10. The same kinetic model results were also obtained for pH 6.8 PBS medium, except that AZM was the best fit model for Hopfenberg.

In vitro release results indicates that the nanoparticles demonstrated a rapid release in the first hour, then showed a controlled release profile. This condition can be associated with the drug amount on the surface of nanoparticles. In both dissolution media, AZM-NP-1:10 exhibited a higher release profile than AZM-NP-1:5 which can be associated with the higher drug loading of AZM-NP-1:10 in comparison with AZM-NP-1:5. Musumeci *et al*. stated in a study that the higher burst effect can be associated with a higher entrapment efficiency [55]. The similarity results indicate that there is no significant difference between the drug release profiles in pH 1.2 and pH 6.8 media for each formulation. The results obtained confirm the pH-independent solubility property of the ERL polymer [58]. The Peppas-Sahlin model, one of the mathematical drug release models, shows Fickian diffusion and erosion of the polymer matrix. In the

first hour, AZM is mainly released from the nanoparticles by Fickian diffusion. It could be stated that the drug transport mechanism of AZM-NP-1:5 was controlled by Fickian diffusion and case II relaxation [59]. Korsmeyer-Peppas model supposes is a combined diffusion and swelling of the polymeric matrix. The n value of Korsmeyer-Peppas model less than 0.5 indicates that the release mechanism is governed by diffusion. This model describes the controlled drug release from a polymeric system, which is compatible with the drug release profile of AZM-NP-1:10 [60-62].

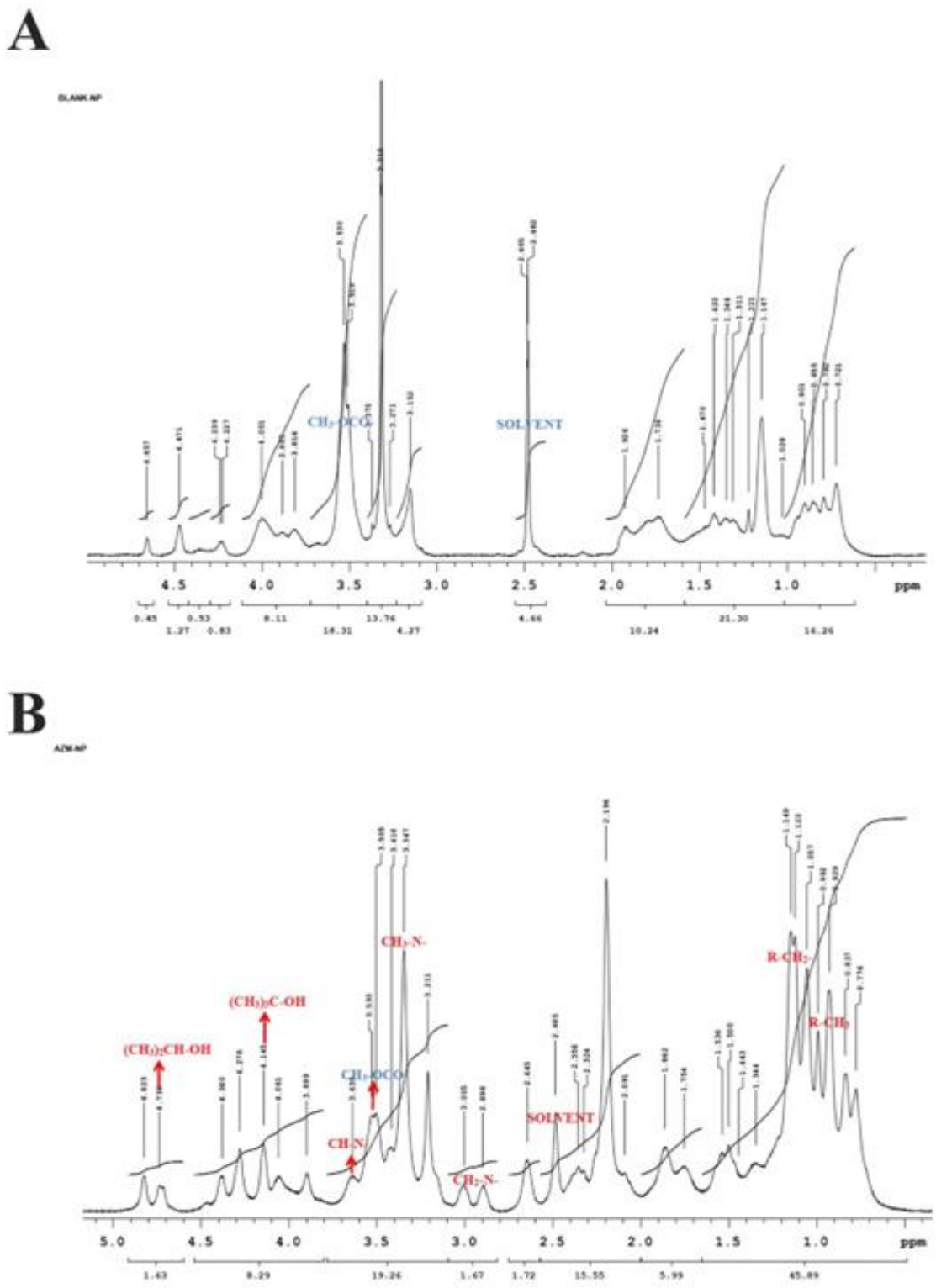

Figure 5.
^{1}H-NMR spectra of Blank-NP (**A**) and AZM-NP-1:10 (**B**)
(peaks assigned in blue: AZM, peaks assigned in red: AZM-NP-1:10)

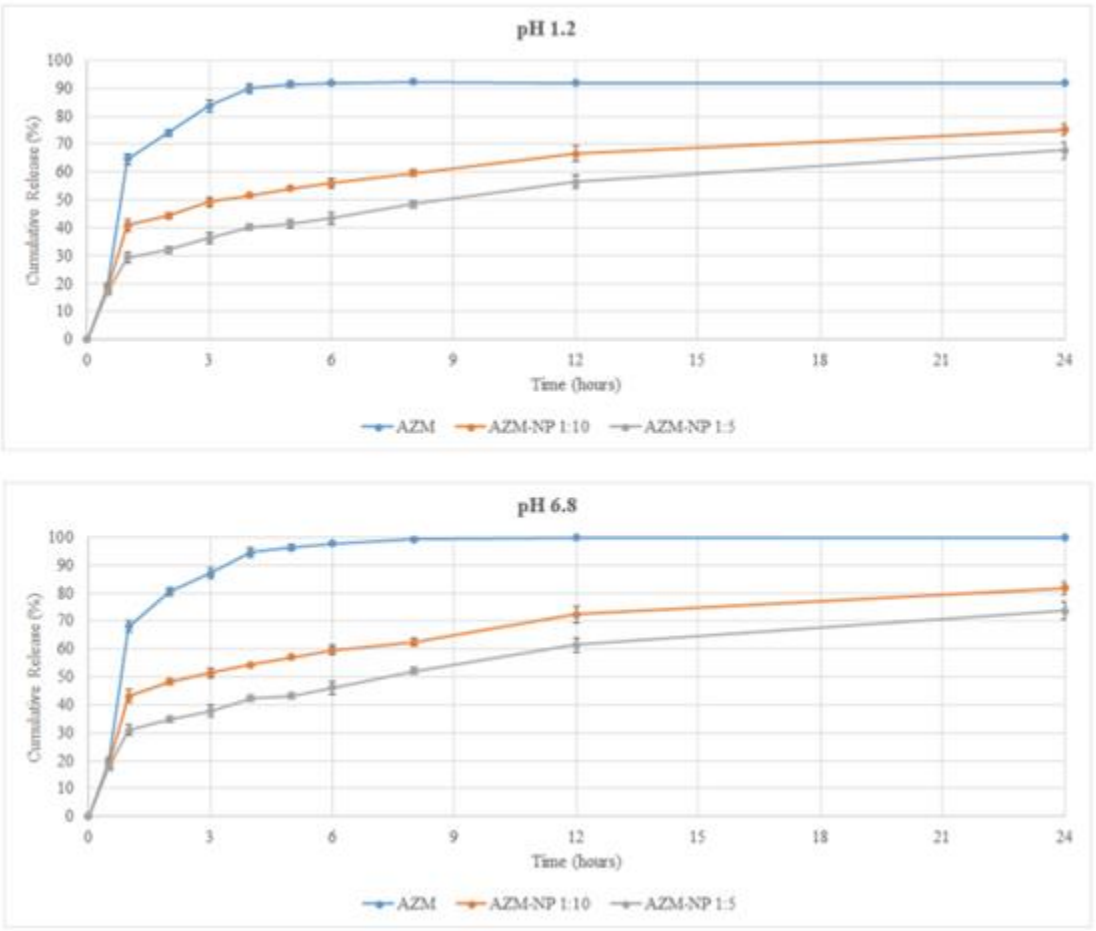

Figure 6.
In vitro release profile of AZM, AZM-NP-1:5 and AZM-NP-1:10 at pH 1.2 HCl and pH 6.8 PBS media (n = 3)

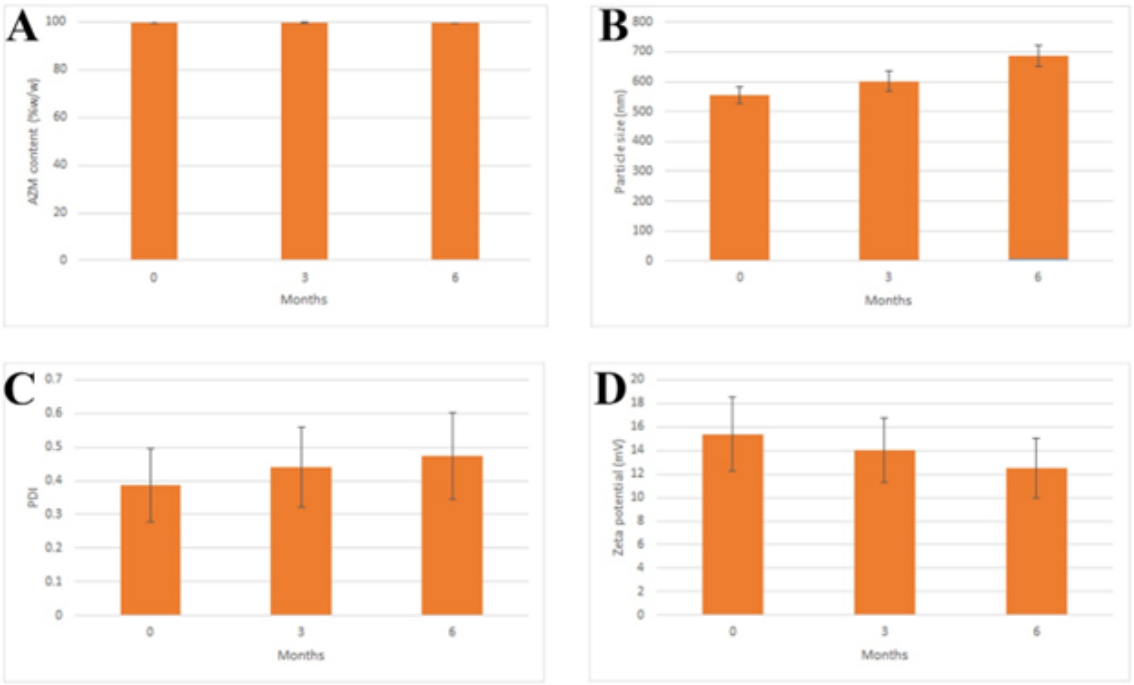

Figure 7.
Storage stability results of AZM-NP-1:10 (n = 3) over 6 months for: (**A**) Azithromycin content (% w/w), (**B**) Particles size (nm), (**C**) PDI and (**D**) Zeta potential (mV)

Storage stability

In this study, AZM-NP-1:10 samples were collected and stored at 30°C ± 2°C/65% RH ± 5% RH conditions in dried form for 0, 3 and 6 months, and azithromycin content in nanoparticles was analysed. The storage stability results presented in Figure 7 revealed that the initial content of 99.78 ± 0.47% was 99.54 ± 0.22% at the end of 3 months and 99.44 ± 0.18% at the end of 6 months with a slight decrease of 0.3%. According to the physical characterization of nanoparticles, while the freshly prepared AZM-NP-1:10 formulation had a zeta potential of 15.4 ± 3.18 mV, it decreased to 12.5 ± 2.51 mV at the end of 6 months. The freshly prepared AZM-NP-1:10 formulation had 554.4 ± 29.3 nm size and 0.387 ± 0.11 PDI. At the end of 6 months the particle size increased to 681.9 ± 36.1 nm and the PDI was 0.474 ± 0.13.

When the obtained storage stability results were examined, it was determined that there was no statistically significant difference between AZM content values in 6-month periods ($p > 0.05$). Similarly, in a study by Ren *et al*., the storage stability of azithromycin-loaded liposomes at room temperature was analysed and no statistically significant difference was found in the azithromycin content of the liposome at the end of the third month compared to the initial content [63]. The increase in particle size and PDI is thought to be associated with particle aggregation. A similar situation has been encountered before [64].

Antibacterial activity evaluation of AZM and nanoparticles

Staphylococcus aureus ATCC 29213 strain was used in this study. EUCAST has published the MIC ranges for quality control strains. According to EUCAST, the MIC range of azithromycin is 0.5 - 2 μg/mL [65]. MIC value of AZM for *S. aureus* ATCC 29213 was found 2 μg/mL in this study. Table III summarizes the MIC values of the formulations based on the broth microdilution test. According to these results, the MIC value of AZM-NP-1:10 was four times lower than the MIC value of AZM for *S. aureus* ATCC 29213. The MIC value of the blank nanoparticle was 1024 μg/mL.

When the antibacterial activity studies conducted with azithromycin nanoparticles were examined in the literature, it was seen that similar results were revealed. Azdarzadeh *et al*. prepared azithromycin nanoparticles with poly(lactic-co-glycolic acid) (PLGA) polymer using the Modified Quasi-Emulsion Solvent Diffusion (MQESD) method. In the study examining antibacterial activity, it was revealed that azithromycin-nanoparticles formed an 8 times lower MIC value compared to the azithromycin MIC value [66]. In another study, Khanmohammadi *et al*. prepared azithromycin nanoparticles with PLGA or Eudragit RS 100 using the MQESD method, and the MIC value of the nanoparticle against *Staphylococcus aureus* ATCC 6538 was 16 times lower in comparison to pure azithromycin [67]. It can be appreciated that the results are in alignment with other studies about the antibacterial activity of AZM-NP-1:10. AZM-NP-1:10 inhibits microbial growth at a lower concentration than non-encapsulated AZM.

Table III

MIC values of formulations against *S. aureus* ATCC 29213 (n = 3)

Formulations	MIC values (μg/mL)
AZM	2
AZM-NP-1:10	0.5
Blank-NP	1024

Time-kill assay

The time-kill curves of AZM, AZM-NP-1:10, Blank-NP and growth control are illustrated in Figure 8. In the time-kill assay, changes in the CFU/mL of bacterial colonies demonstrate the bactericidal activity of the formulations. The most significant result was obtained at the MIC concentration. According to the time-kill results, the activity of AZM started to decrease after the 4th hour and showed a dramatic decrease after the 6th hour. However, AZM-NP-1:10 showed continuous antibacterial activity for 24 hours.

Based on the time-kill data, AZM-NP-1:10 successfully induced the long-term controlled release of azithromycin. Since the antibacterial activity of blank nanoparticles was almost non-existent, it was given results in parallel with the growth control. In the study of Mushtaq *et al*., it was observed that the blank nanoparticles did not show antibacterial activity [68]. In addition, similar results about Blank-NP were also observed in the study conducted by Scolari *et al*. In this research, Rifampicin-loaded alginate/chitosan nanoparticles were examined against *Staphylococcus aureus*. The blank nanoparticles did not indicate an antibacterial effect against *S. aureus* ATCC 29213 [69].

S. aureus can live intracellularly in phagocytes causing recurrent infections and causing host cell death. The long-term release feature of the nanoparticle may provide an alternative approach to the treatment of infectious diseases by enabling it to show intracellular activity. Nirbhavane *et al*. prepared solid lipid nano-particles (SLN) using the solvent diffusion evaporation method. In the time-kill results, azithromycin SLN corroborated a sustained antibacterial activity against *S. aureus* 22359 [70]. Figure 8 indicates a 1.5 log10 decrease in cell viability in the colony treated with AZM-NP-1:10. Mushtaq *et al*. reported that the ceftriaxone-loaded chitosan nanoparticles caused an ~ 1 log10 decrease in the viability of Methicillin-resistant *S. aureus* [68].

According to the obtained results, the prepared AZM-NP-1:10 formulation showed an effective enhancement in the antibacterial efficiency against *S. aureus* ATCC 29213. AZM-NP-1:10 is more effective than AZM during an extended period. Thus AZM-NP-1:10 is a

favourable formulation for prolonged and continuous antibacterial activity.

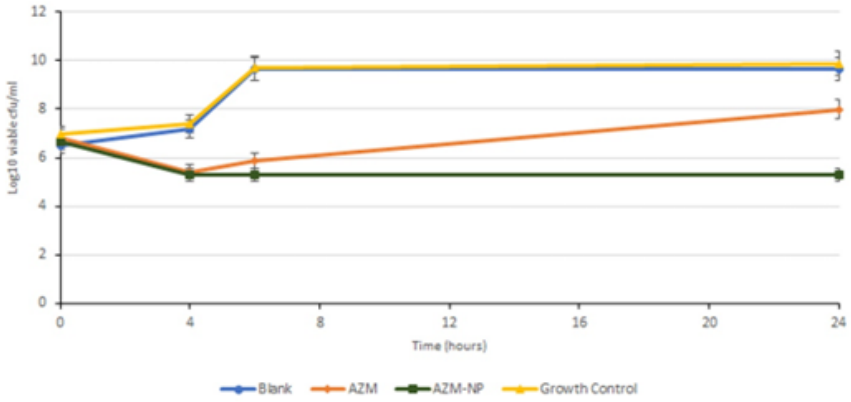

Figure 8.
Time-kill results for *S. aureus* ATCC 29213 (n = 3)

Conclusions

In this study, AZM a macrolide antibiotic was successfully loaded into nanoparticles using ERL polymer as a novel approach to obtain extended antibacterial activity. The time-kill assay showed that AZM-NP-1:10 effectively inhibited the growth of *Staphylococcus aureus* ATCC 29213 for 24 hours compared to free AZM due to the prolonged-release characteristics of nanoparticles. To conclude, AZM-loaded nanoparticles promoted a remarkably effective and long-term antibacterial activities. The AZM nanoparticles were designed as a promising drug delivery system for the treatment of bacterial infections. Further studies are necessary to evaluate the pharmacological activity of formulation in animal models.

Conflict of interest

The authors declare no conflict of interest.

References

1. Rodrigues GR, López-Abarrategui C, de la Serna Gómez I, Dias SC, Otero-González AJ, Franco OL, Antimicrobial magnetic nanoparticles based-therapies for controlling infectious diseases. *Int J Pharm.*, 2019; 555: 356-367.
2. Lee NY, Ko WC, Hsueh PR, Nanoparticles in the Treatment of Infections Caused by Multidrug-Resistant Organisms. *Front Pharmacol.*, 2019; 10: 1153.
3. Chokshi A, Sifri Z, Cennimo D, Horng H, Global contributors to antibiotic resistance. *J Glob Infect Dis.*, 2019; 11(1): 36-42.
4. The Review on Antimicrobial Resistance (Chaired by Jim O'Neill). Tackling Drug-Resistant Infections Globally: Final Report and Recommendations, 2016.
5. Scarafile G, Antibiotic resistance: current issues and future strategies. *Rev Health Care*, 2016; 7(1): 3-16.
6. Antimicrobial Resistance: Global Report on Surveillance. World Health Organization, 2014.
7. Global Antimicrobial Resistance Surveillance System (GLASS) Report: Early Implementation 2020. World Health Organization, 2020.
8. Allahverdiyev AM, Kon KV, Abamor ES, Bagirova M, Rafailovich M, Coping with antibiotic resistance: combining nanoparticles with antibiotics and other antimicrobial agents. *Exp Rev Anti-Infective Ther.*, 2011; 9(11): 1035-1052.
9. Valizadeh H, Mohammadi G, Ehyaei R, Milani M, Azhdarzadeh M, Zakeri-Milani P, Lotfipour F, Antibacterial activity of clarithromycin loaded PLGA nanoparticles. *Pharmazie*, 2012; 67(1): 63-68.
10. Canaparo R, Foglietta F, Giuntini F, Della Pepa C, Dosio F, Serpe L, Recent developments in antibacterial therapy: Focus on stimuli-responsive drug-delivery systems and therapeutic nanoparticles. *Molecules*, 2019; 24(10): 1991.
11. Vauthier C, Bouchemal K, Methods for the Preparation and Manufacture of Polymeric Nanoparticles. *Pharm Res.*, 2009; 26(5): 1025-1058.
12. Cooper DL, Conder CM, Harirforoosh S, Nanoparticles in drug delivery: mechanism of action, formulation and clinical application towards reduction in drug-associated nephrotoxicity. *Expert Opin Drug Deliv.*, 2014; 11(10): 1661-1680.
13. Nava-Arzaluz MG, Pinon-Segundo E, Ganem-Rondero A, Lechuga-Ballesteros D, Single emulsion-solvent evaporation technique and modifications for the preparation of pharmaceutical polymeric nanoparticles. *Recent Pat Drug Deliv Formul.*, 2012; 6(3): 209-223.
14. Zielinska A, Carreiró F, Oliveira AM, Neves A, Pires B, Venkatesh DN, Durazzo A, Lucarini M, Eder P, Silva AM, Santini A, Souto EB, Polymeric nanoparticles: production, characterization, toxicology and ecotoxicology. *Molecules*, 2020; 25(16): 3731.
15. Sánchez A, Mejía SP, Orozco J, Recent Advances in Polymeric Nanoparticle-Encapsulated Drugs against Intracellular Infections. *Molecules*, 2020; 25(16): 3760.
16. Salatin S, Barar J, Barzegar-Jalali M, Adibkia K, Kiafar F, Development of a nanoprecipitation method for the entrapment of a very water soluble drug into

Eudragit RL nanoparticles. *Res Pharm Sci.*, 2017; 12(1): 1-14.
17. Singh G, Pai RS, Atazanavir-loaded Eudragit RL 100 nanoparticles to improve oral bioavailability: Optimization and *in vitro*/*in vivo* appraisal. *Drug Deliv.*, 2016; 23(2): 532-539.
18. McMullan BJ, Mostaghim M, Prescribing azithromycin. *Aust Presc.*, 2015; 38(3): 87-90.
19. Dinos GP, The macrolide antibiotic renaissance. *Br J Pharmacol.*, 2017; 174(18): 2967-2983.
20. World Health Organisation. Critically Important Antimicrobials for Human Medicine 6th Revision 2018. Ranking of medically important antimicrobials for risk management of antimicrobial resistance due to non-human use.
21. Milić A, Mihaljević VB, Ralić J, Bokulic A, Nozinic D, Tavcar B, Mildner B, Munic V, Malnar I, Padovan J, A comparison of *in vitro* ADME properties and pharmacokinetics of azithromycin and selected 15-membered ring macrolides in rodents. *Eur J Drug Metab Pharmacokinet.*, 2014; 39(4): 263-276.
22. Zuckerman JM, Macrolides and ketolides: Azithromycin, clarithromycin, telithromycin. *Infect Dis Clin North Am.*, 2004; 18(3): 621-649.
23. Ghari T, Mortazavi SA, Khoshayand MR, Kobarfard F, Gilani K, Preparation, optimization, and *in vitro* evaluation of azithromycin encapsulated nanoparticles by using response surface methodology. *J Drug Deliv Sci Technol.*, 2014; 24(4): 352-360.
24. Firth A, Prathapan P, Azithromycin: The First Broad-spectrum Therapeutic. *Eur J Med Chem.*, 2020; 207: 112739.
25. Tran P, Park JS, Recent trends of self-emulsifying drug delivery system for enhancing the oral bioavailability of poorly water-soluble drugs. *J Pharm Invest.*, 2021; 51: 439-463.
26. Buya AB, Beloqui A, Memvanga PB, Préat V, Self-nano-emulsifying drug-delivery systems: From the development to the current applications and challenges in oral drug delivery. *Pharmaceutics*, 2020; 12: 1194.
27. Adibkia K, Khorasani G, Payab S, Lotfipour F, Anti *pneumococcal* activity of azithromycin-Eudragit RS100 nano- formulations. *Adv Pharm Bull.*, 2016; 6(3): 455-459.
28. Payab S, Jafari-Aghdam N, Barzegar-Jalali M, Mohammadi G, Lotfipour F, Gholikhani T, Adibkia K, Preparation and physicochemical characterization of the azithromycin-Eudragit RS100 nanobeads and nanofibers using electrospinning method. *J Drug Deliv Sci Technol.*, 2014; 24(6): 585-590.
29. Taghe S, Mirzaeei S, Alany RG, Nokhodchi A, Polymeric inserts containing Eudragit® L100 nano-particle for improved ocular delivery of azithromycin. *Biomedicines*, 2020; 8(11): 1-21.
30. Assi RA, Darwis Y, Abdulbaqi IM, Asif SM, Development and validation of a stability-indicating RP-HPLC method for the detection and quantification of azithromycin in bulk, and self-emulsifying drug delivery system (SEDDs) formulation. *J Appl Pharm Sci.*, 2017; 7(9): 20-29.
31. European Medicines Agency. ICH Topic Q 1 A (R2) Stability Testing of new Drug Substances and Products. www.ema.europa.eu/en/documents/scientific-guide-line/ich-q-1-r2-stability-testing-new-drug-substances-products-step-5_en.pdf, 2022. www.emea.eu.int.
32. Paramera EI, Konteles SJ, Karathanos VT, Stability and release properties of curcumin encapsulated in *Saccharomyces cerevisiae*, β-cyclodextrin and modified starch. *Food Chem.*, 2011; 125(3): 913-922.
33. Balouiri M, Sadiki M, Ibnsouda SK, Methods for *in vitro* evaluating antimicrobial activity: A review. *J Pharm Anal.*, 2016; 6(2): 71-79.
34. Yeo Y, Park K, Control of encapsulation efficiency and initial burst in polymeric microparticle systems. *Arch Pharm Res.*, 2004; 27(1): 1-12.
35. Patil PS, Dhawale SC, Development of ritonavir loaded nanoparticles: *In vitro* and *in vivo* characterization. *Asian J Pharm Clin Res.*, 2018; 11(3): 284-288.
36. Choi NW, Verbridge SS, Williams RM, Chen J, Kim YJ, Schmehl R, Farnum CE, Zipfel WR, Fischbach C, Stroock AD, Phosphorescent nanoparticles for quantitative measurements of oxygen profiles *invitro* and *invivo*. *Biomaterials*, 2012; 33(9): 2710-2722.
37. Park MH, Baek JS, Lee CA, Kim DC, Cho CW, The effect of Eudragit type on BSA-loaded PLGA nanoparticles. *J Pharm Invest.*, 2014; 44: 339-349.
38. Heurtault B, Saulnier P, Pech B, Proust JE, Benoit JP, Physico-chemical stability of colloidal lipid particles. *Biomaterials*, 2003; 24(23): 4283-4300.
39. Sahana DK, Mittal G, Bhardwaj V, Kumar MNVR, PLGA nanoparticles for oral delivery of hydrophobic drugs: Influence of organic solvent on nanoparticle formation and release behavior *in vitro* and *in vivo* using estradiol as a model drug. *J Pharm Sci.*, 2008; 97(4): 1530-1542.
40. Soltani S, Zakeri-Milani P, Barzegar-Jalali M, Jelvehgari M, Design of eudragit RL nanoparticles by nanoemulsion method as carriers for ophthalmic drug delivery of ketotifen fumarate. *Iran J Basic Med Sci.*, 2016; 19(5): 850-860.
41. Monika P, Basavaraj BV, Chidambara Murthy KN, Ahalya N, Bharath S, Enrichment of *in vivo* efficacy of catechin rich extract with the application of nanotechnology. *Int J Appl Pharm.*, 2018; 10(5): 281-288.
42. Hari BNV, Narayanan N, Dhevendaran K, Ramyadevi D, Engineered nanoparticles of Efavirenz using methacrylate co-polymer (Eudragit-E100) and its biological effects *in-vivo*. *Mat Sci Engin C.*, 2016; 67: 522-532.
43. Timoumi S, Mangin D, Peczalski R, Zagrouba F, Andrieu J, Stability and thermophysical properties of azithromycin dihydrate. *Arab J Chem.*, 2014; 7(2): 189-195.
44. Koopaei MN, Maghazei MS, Mostafavi SH, Jamalifar H, Samadi N, Amini M, Malek SJ, Darvishi B, Atyabi F, Dinarvand R, Enhanced antibacterial activity of roxithromycin loaded pegylated poly lactide-co-glycolide nanoparticles. *DARU.*, 2012; 20(1): 92.
45. Gambhire VM, Salunkhe SM, Gambhire MS, Atorvastatin-loaded lipid nanoparticles: antitumor activity studies on MCF-7 breast cancer cells. *Drug Dev Ind Pharm.*, 2018; 44(10): 1685-1692.
46. Sapsford KE, Tyner KM, Dair BJ, Deschamps JR, Medintz IL, Analyzing Nanomaterial Bioconjugates: A Review of Current and Emerging Purification and

Characterization Techniques. *Anal Chem.*, 2011; 83(12): 4453-4488.
47. Katla VM, Veerabrahma K, Cationic solid self micro emulsifying drug delivery system (SSMED) of losartan: Formulation development, characterization and *in vivo* evaluation. *J Drug Deliv Sci Tech.*, 2016; 35: 190-199.
48. Kumar N, Chaurasia S, Patel RR, Khan G, Kumar V, Mishra B, Atorvastatin calcium encapsulated eudragit nanoparticles with enhanced oral bioavailability, safety and efficacy profile. *Pharm Dev Technol.*, 2015; 22(2): 156-167.
49. Verma P, Gupta RN, Jha AK, Pandey R, Development, *in vitro* and *in vivo* characterization of Eudragit RL 100 nanoparticles for improved ocular bioavailability of acetazolamide. *Drug Deliv.*, 2013; 20(7): 269-276.
50. Pagar K, Vavia P, Rivastigmine-loaded L-lactide-depsipeptide polymeric nanoparticles: Decisive formulation variable optimization. *Sci Pharm.*, 2013; 81(3): 865-885.
51. Dikmen G, Guney G, Genc L, Characterization of solid lipid nanoparticles containing caffeic acid and determination of its effects on MCF-7 cells. *Recent Pat Anticancer Drug Discov.*, 2015; 10(2): 224-232.
52. Gil RR, Constitutional, configurational, and conformational analysis of small organic molecules on the basis of NMR residual dipolar couplings. *Angew Chem Int Ed Engl.*, 2011; 50(32): 7222-7224.
53. Tung NT, Tran CS, Nguyen TL, Hoang T, Trinh TD, Nguyen TN, Formulation and biopharmaceutical evaluation of bitter taste masking microparticles containing azithromycin loaded in dispersible tablets. *Eur J Pharm Biopharm.*, 2018; 126: 187-200.
54. Bhagav P, Upadhyay H, Chandran S, Brimonidine tartrate-eudragit long-acting nanoparticles: Formulation, optimization, *in vitro* and *in vivo* evaluation. *AAPS PharmSciTech.*, 2011; 12(4): 1087-1101.
55. Musumeci T, Ventura CA, Giannone I, Ruozi B, Montenegro L, Pignatello R, Puglisi G, PLA/PLGA nanoparticles for sustained release of docetaxel. *Int J Pharm.*, 2006; 325(1-2): 172-179.
56. Muselík J, Komersová A, Kubová K, Matzick K, Skalická B, A Critical Overview of FDA and EMA Statistical Methods to Compare *In Vitro* Drug Dissolution Profiles of Pharmaceutical Products. *Pharmaceutics*, 2021; 13(10): 1703.
57. Kulpreechanan N, Sorasitthiyanukarn FN, Evaluation of *in vitro* release kinetics of capsaicin-loaded chitosan nanoparticles using DDsolver. *Int J Res Pharm Sci.*, 2020; 11: 4555-4559.
58. Thakral S, Thakral NK, Majumdar DK, Eudragit: a technology evaluation. *Exp Opin Drug Deliv.*, 2013; 10(1): 131-149.
59. Unagolla JM, Jayasuriya AC, Drug transport mechanisms and *in vitro* release kinetics of vancomycin encapsulated chitosan-alginate polyelectrolyte microparticles as a controlled drug delivery system. *Eur J Pharm Sci.*, 2018; 114: 199-209.
60. Permanadewi I, Kumoro AC, Wardhani DH, Aryanti N, Modelling of controlled drug release in gastro-intestinal tract simulation. *J Physics: Conf Series*, 2019; 1295: 012063.
61. Shabbir M, Ali S, Hamid I, Sharif A, Akhtar MF, Raza M, Ahmed S, Peerzada S, Amin MU, Influence of different formulation variables on the performance of transdermal drug delivery system containing tizanidine hydrochloride: *In vitro* and *ex vivo* evaluations. *Braz J Pharm Sci.*, 2018; 54(04): e00130.
62. Arora G, Malik K, Singh I, Formulation and evaluation of mucoadhesive matrix tablets of taro gum: optimization using response surface methodology. *Polim Med.*, 2011; 41(2): 23-34.
63. Ren T, Lin X, Zhang Q, You D, Liu X, Tao X, Gou J, Zhang Y, Yin T, He H, Tang X, Encapsulation of Azithromycin Ion Pair in Liposome for Enhancing Ocular Delivery and Therapeutic Efficacy on Dry Eye. *Mol Pharm.*, 2018; 15(11): 4862-4871.
64. Lütfi G, Müzeyyen D, Preparation and characterization of polymeric and lipid nanoparticles of pilocarpine HCl for ocular application. *Pharm Dev Technol.*, 2013; 18(3): 701-709.
65. EUCAST. European Committee on Antimicrobial Susceptibility Testing - Routine and extended internal quality control for MIC determination and disk diffusion as recommended by EUCAST. Version 12.0 2022: 1-23.
66. Azhdarzadeh M, Lotfipour F, Zakeri-Milani P, Mohammadi G, Valizadeh H, Anti-bacterial performance of azithromycin nanoparticles as colloidal drug delivery system against different gram-negative and gram-positive bacteria. *Adv Pharm Bull.*, 2012; 2(1): 17-24.
67. Khanmohamadi H, Antibacterial evaluation of azithromycin nanoparticles. 13th Iranian Pharmaceutical Sciences Congress, 2012; 7(5): 14.
68. Mushtaq S, Khan JA, Rabbani F, Latif U, Arfan M, Yameen MA, Biocompatible biodegradable polymeric antibacterial nanoparticles for enhancing the effects of a third-generation cephalosporin against resistant bacteria. *J Med Microbiol.*, 2017; 66(3): 318-327.
69. Radu IC, Hudiță A, Zaharia C, Negrei C, Burcea Dragomiroiu GTA, Popa DE, Costache M, Iovu H, Georgescu M, Ginghină O, Gălățeanu B, Silk fibroin nanoparticles reveal efficient delivery of 5-FU in a HT-29 colorectal adenocarcinoma model *in vitro*. *Farmacia*, 2021; 69(1): 113-122.
70. Nirbhavane P, Vemuri N, Sharma K, Jain S, Krishan Khuller G, Nano-Lipoidal Azithromycin: A Strategy to Improve the Antimicrobial Performance of the Drug. *Nanomed Nanotech J.*, 2022; 3(1): 128.